Citation: Molecular Therapy — Oncolytics (2015) **2,** 15003; doi:10.1038/mto.2015.3

www.nature.com/mto

ARTICLE

Expression of anti-VEGF antibody together with anti-EGFR or anti-FAP enhances tumor regression as a result of vaccinia virotherapy

Ting Huang[1], Huiqiang Wang[2], Nanhai G Chen[2,3], Alexa Frentzen[2], Boris Minev[2-4] and Aladar A Szalay[1–3]

The tumor microenvironment plays an important role in tumor growth and progression. Here we demonstrate that vaccinia virus-mediated, constitutively expressed intratumoral antibodies against vascular endothelial growth factor (VEGF), epidermal growth factor receptor (EGFR), and fibroblast activation protein (FAP) significantly improved tumor regression and oncolytic virotherapy through suppression of angiogenesis, cell proliferation, and stromagenesis in virus-colonized tumors. In contrast to the tumor growth inhibition by the three tumor growth-inhibiting antibodies individually, when two of the three antibodies were expressed simultaneously by single vaccinia virus strains tumor regression was further enhanced. These findings strongly indicate that interference with the two tumor growth-stimulating mechanisms did in fact result in enhanced therapeutic efficacy in tumor xenograft models and may lead to an effective therapy in patients with cancer.

Molecular Therapy — Oncolytics (2015) **2**, 15003; doi:10.1038/mto.2015.3; published online 18 March 2015

INTRODUCTION

In spite of great advances in anticancer treatments over the past 30 years, cancer remains the leading cause of death around the world. Overlooking the important role of tumor microenvironment (TME) in cancer growth and metastasis may be one of the reasons.[1,2] Angiogenesis and hyper-proliferation of cells in the stroma of tumors not only support the growth of cancer but also contribute to its development, for example, metastasis. Therefore, combining therapies that target cancer cells and the TME should result in greater therapeutic benefits than most of the current therapies that target cancer cells only. Factors within the TME such as vascular endothelial growth factor (VEGF), epidermal growth factor receptor (EGFR), and fibroblast activation protein (FAP) play crucial roles in cancer initiation and development.[3–5] The high-level expression of VEGF or EGFR correlates with poor prognosis in patients with breast, colon, lung, head and neck, and other cancers.[6,7] The anti-VEGF monoclonal antibody (mAb), bevacizumab (Avastin), was approved by the US Food and Drug Administration (FDA) in 2004 for the treatment of metastatic colon cancer and subsequently other metastatic cancers. In the same year, anti-EGFR mAb, cetuximab (Erbitux), was also approved by the FDA for the treatment of metastatic colon cancer. However, the clinical efficacy of Avastin and Erbitux has been somewhat limited[8–10] possibly due to poor tumor penetration and rapid clearance of the mAbs from the circulation, requiring the administration of high doses at frequent intervals and extensive durations, also making the therapies extremely costly.[11]

Improvements in the pharmacodynamic properties of current mAb therapeutics and identification of additional functionalities targeting the TME could be greatly beneficial. For example, G6-31 is an improved anti-VEGF antibody derived from a phage display library with better binding affinity and enhanced therapeutic efficacy in animal models than Avastin.[12] To improve tumor penetration, a single-domain antibody of 15 kDa against EGFR from a llama has been recently developed (termed anti-EGFRVHH).[13,14] This llama nanobody was nonimmunogenic in mice and was proven to block binding of EGF to EGFR, thereby inhibiting EGFR signaling and showing the specific tumor targeting.[15,16] Anti-EGFRVHH is used for molecular imaging and therapeutic applications.[14,17–19] FAP (also known as seprase), a highly conserved protein, is richly expressed particularly in the stroma of aggressive cancers.[20–22] The high-level expression of FAP is correlated with cancer progression.[23–25] To date, no specific molecular inhibitor of FAP has been developed.[4,26] M036, a species-cross-reactive FAP-specific single-chain antibody (scAb), was isolated by sequential phage display and was shown to bind FAP on stromal cells of different human carcinomas and the murine host stroma in human tumor xenografts.[27] The therapeutic potential of M036 has not yet been evaluated.

Combining the TME-targeted antiangiogenic and antiproliferative activities of these antibodies with a potent anticancer therapeutic in a form that could be simultaneously and efficiently administered was the goal of this research. The replication-competent oncolytic vaccinia virus (VACV) GLV-1h68 locates,

[1]Department of Biochemistry, Rudolph Virchow Center for Experimental Biomedicine, Institute for Molecular Infection Biology, University of Würzburg, Würzburg, Germany; [2]Genelux Corporation, San Diego Science Center, San Diego, California, USA; [3]Department of Radiation Medicine and Applied Sciences, Rebecca & John Moores Comprehensive Cancer Center, University of California, San Diego, California, USA; [4]Division of Neurosurgery, University of California, San Diego, California, USA. Correspondence: AA Szalay (aaszalay@aol.com)
Received 12 December 2014; accepted 20 December 2014

replicates, and lyses tumor cells in human xenograft nude mouse models after administration of a single dose.[28] GLV-1h68 is currently in phase 1/2 clinical trials for the treatment of solid tumors. Additionally, recombinant VACVs can be genetically modified to express functional transgenes, including scAbs. We showed previously that VACVs expressing the anti-VEGF scAb GLAF-1, designed according to the sequence of G6-31,[12] significantly improved anticancer therapeutic efficacy in mice compared with the parental virus, GLV-1h68.[29] The therapeutic efficacy was further enhanced in combination with radiation therapy.[30]

Thus, we constructed and tested new recombinant VACVs expressing novel TME-targeted antiproliferative activities by encoding a scAb against FAP (GLV-1h282) and a single-domain antibody against EGFR (GLV-1h442). VACVs expressing these individual antibodies significantly suppressed tumor growth in xenograft tumor models, verifying the functionality and therapeutic activity of the virally expressed antibodies. Lastly, we created additional recombinant VACVs encoding two antibodies with both antiproliferative and antiangiogenic activities targeting VEGF and EGFR (GLV-1h444) or VEGF and FAP (GLV-1h446). The new VACVs expressing the TME-targeted antibodies, either singly or in combination, significantly enhanced the antitumor efficacy of oncolytic virotherapy. Moreover, treatment of tumors in mice with the two antibody-expressing VACVs, GLV-1h444 or GLV-1h446, was superior to the concomitant treatment with GLV-1h68 in combination with continuous administration of Avastin and Erbitux. The antiproliferative and antiangiogenic effects of the virally expressed antibodies were also apparent in tumors beyond the areas directly infected by the virus, demonstrating that the scAbs are capable of tumor permeation, while locally expressed. Thus, our results demonstrated that oncolytic virotherapy with VACV was significantly enhanced by coexpression of virus-encoded antibodies with antiproliferative and antiangiogenic activities targeting the TME. Additionally, the enhanced treatment effects were achieved by a single administration of the replication-competent, recombinant VACVs.

RESULTS

Construction of recombinant VACVs encoding individual antibodies targeting EGFR and FAP

We previously showed that an anti-VEGF scAb (GLAF-1 or GLAF-2) expressed by VACVs (GLV-1h108 (ref. 29) and GLV-1h164 (ref. 30)) significantly reduced tumor growth in several human tumor xenograft models and exhibited "Avastin-like mode of action" through the inhibitory effects on vascularity in the TME. EGFR and FAP are other important factors in the TME that are involved in the regulation of tumor initiation and development.[4,7] To evaluate the effect of antibodies targeting EGFR and FAP on the therapeutic efficacy of oncolytic virotherapy, two new recombinant VACVs were constructed by replacing the *lacZ* expression cassette at the *J2R* locus of GLV-1h68 with an anti-EGFR nanobody (anti-EGFRVHHFLAG) expression cassette or with an anti-FAP scAb (GLAF-5) expression cassette, both under the control of the VACV synthetic early/late (PSEL) promoter, resulting in GLV-1h442 and GLV-1h282, respectively (Figure 1a,b).

Virally expressed antibodies targeting VEGF, EGFR, and FAP significantly enhance virotherapy

The antitumor effect of treatment with VACV strains encoding anti-VEGF, anti-FAP scAbs, or anti-EGFR nanobody was investigated in mice. The VACV strains or PBS (phosphate-buffered saline) was injected retro-orbitally at a single dose of 2×10^6 plaque-forming units (PFU)/mouse into mice bearing different human tumor xenografts. Avastin or Erbitux was administered to mice twice weekly by intraperitoneal (i.p.) injection for a period of 5 weeks beginning 10 days after virus injection (as indicated by arrows in Figure 2a–c). In the A549 xenograft model ($n \geq 7$) (Figure 2a,b), PBS-treated tumors

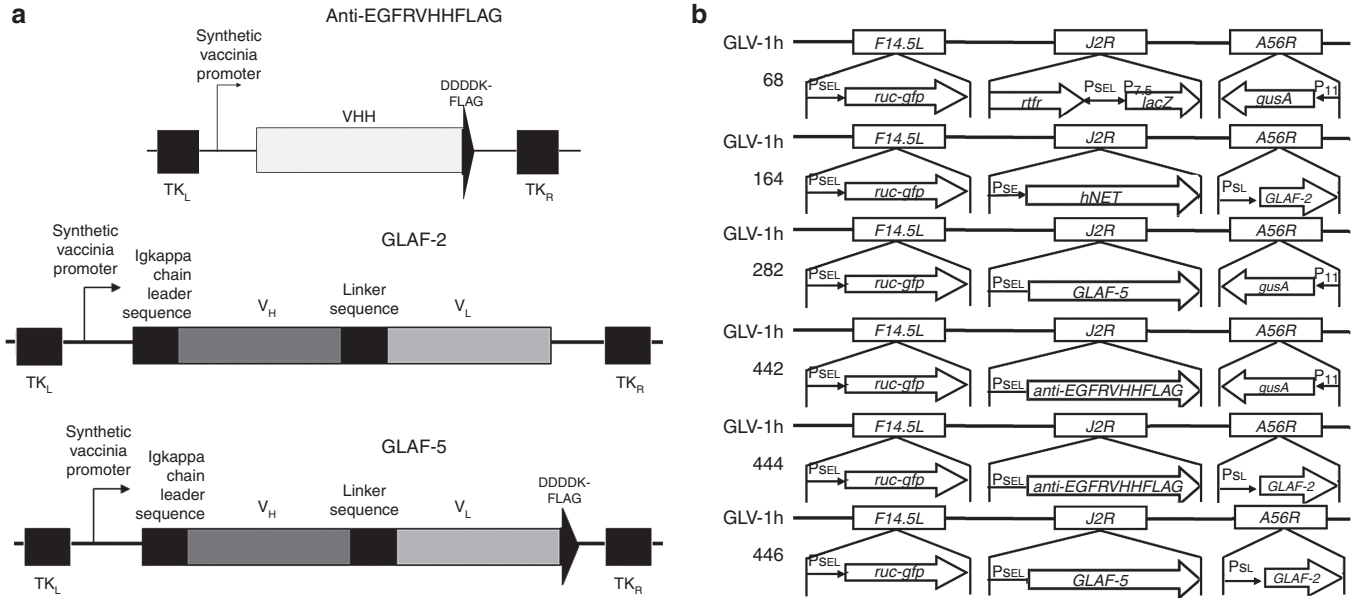

Figure 1 A schematic representation of antibodies and the new VACVs. (**a**) Schematic diagrams of anti-EGFRVHHFLAG, anti-VEGF scAb (GLAF-2), and anti-FAP scAb (GLAF-5) constructs. (**b**) Genomic structures of the new recombinant VACVs along with their parental virus. GLV-1h442 and GLV-1h282 were derived from GLV-1h68 by replacing the *lacZ* expression cassette at the *J2R* locus with the anti-EGFRVHHFLAG and GLAF-5 cassettes, respectively, each under the control of the PSEL promoter. GLV-1h164 was derived from GLV-1h68 by replacing the *lacZ* expression cassette at the *J2R* locus with the *hNET* under the PSE promoter and the *gusA* expression cassette at *A56R* locus with the GLAF-2 cassette under the PSL promoter. GLV-1h444 and GLV-1h446 were derived from GLV-1h164 by replacing the *hNET* expression cassette at the *J2R* locus with the anti-EGFRVHHFLAG and the GLAF-5 expression cassette, respectively, each under the control of the VACV PSEL promoter. All viruses contain the *ruc-gfp* expression cassette at the *F14.5L* locus. PSE, PSEL, PSL, P11, and P7.5 are VACV synthetic early, synthetic early/late, synthetic late, 11K, and 7.5K promoters, respectively.

showed continuous growth until mice had to be sacrificed due to excessive tumor burden. The typical three-phase growth pattern of tumors in mice treated with GLV-h168 was observed, as previously described.[28] The tumor volume exceeded the PBS-treated group at the beginning, followed by significant tumor growth arrest and then continuous tumor shrinkage. Mice treated with Avastin alone exhibited a reduction in tumor volume compared with PBS, but tumor growth was continuous (Figure 2a). The treatment with GLV-1h68 in combination with Avastin yielded improved efficacy over either treatment alone whereas the therapeutic efficacy of GLV-1h164, expressing anti-VEGF scAb, was comparable to that of GLV-1h68 in combination with Avastin. The treatment with GLV-1h68 in combination with Erbitux yielded smaller tumors than the treatment with GLV-1h68 alone during the period of Erbitux administration, but tumor volume rebounded transiently after the treatment with Erbitux was ceased (Figure 2b). In contrast, tumor growth in mice treated with GLV-1h442, expressing anti-EGFR nanobody, was consistently slower than in mice treated with GLV-1h68, and no rebound

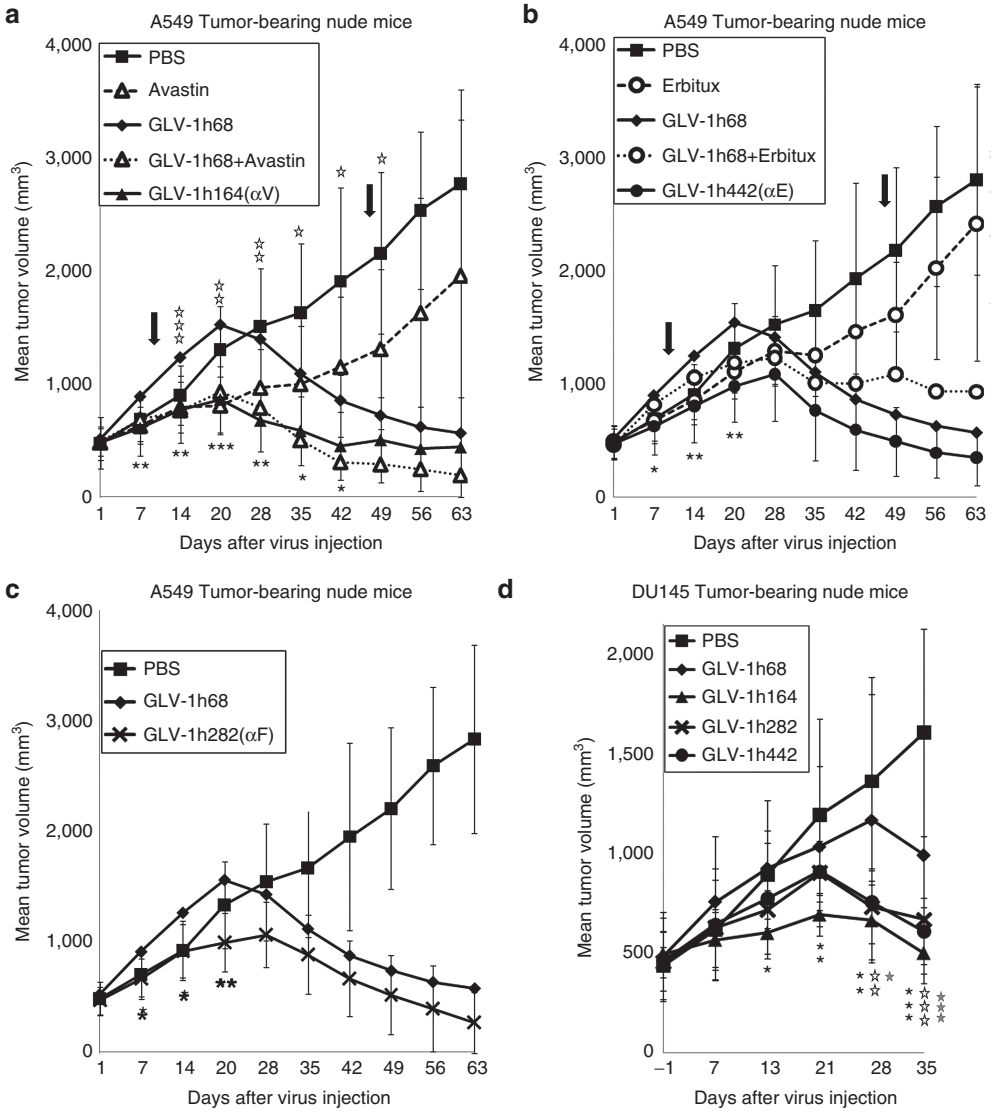

Figure 2 Virally expressed individual therapeutic antibodies targeting the TME significantly enhance virotherapy in A549 and DU145 tumor xenograft models. (**a**) Antibody targeting VEGF expressed from GLV-1h164 significantly enhanced virotherapy. Mice bearing A549 xenograft tumors ($n \geq 7$) were treated with virus alone, Avastin alone, PBS alone, or virus in combination with Avastin. A single dose of virus (2×10^6 pfu/mouse) was given intravenously (i.v.) when tumor volumes reached 450 mm^3. Avastin was administered i.p. at a dose of 5 mg/kg, twice per week for 5 weeks, starting at 10 dpi. The arrows indicate the beginning and end of Avastin treatment. Statistical analysis was performed using one-way ANOVA (***$P < 0.001$, **$P < 0.01$, *$P < 0.05$). Stars indicate the comparison of the GLV-1h68 group with the GLV-1h164 group (black) and with the GLV-1h68+Avastin group (open). αV indicates anti-VEGF. (**b**) Antibody targeting EGFR expressed from GLV-1h442 significantly enhanced virotherapy. Mice bearing A549 xenograft tumors ($n \geq 7$) were treated with virus alone, Erbitux alone, PBS alone, or virus in combination with Erbitux. A single dose of virus (2×10^6 pfu/mouse) was given i.v. when tumor volumes reached 450 mm^3. Erbitux was administered i.p. at a dose of 3 mg/kg, twice per week for 5 weeks, starting at 10 dpi. The arrows indicate the beginning and end of Erbitux treatment. Statistical analysis was performed using one-way ANOVA (**$P < 0.01$, *$P < 0.05$). Stars indicate the comparison of the GLV-1h68 group with the GLV-1h442 group. αE indicates anti-EGFR. (**c**) Antibody targeting FAP expressed from GLV-1h282 significantly enhanced virotherapy. Mice bearing A549 xenograft tumors ($n \geq 7$) were injected i.v. with a single dose of GLV-1h68 or GLV-1h282 (2×10^6 pfu/mouse) when tumor volumes reached 450 mm^3. Statistical analysis was performed using one-way ANOVA (**$P < 0.01$, *$P < 0.05$). Stars indicate the comparison of the GLV-1h68 group with the GLV-1h282 group. αF indicates anti-FAP. (**d**) DU145 tumor-bearing mice ($n = 5$) were injected i.v. with each VACV strain (2×10^6 pfu/mouse) when tumor volumes reached 450 mm^3, and tumor volumes were monitored weekly thereafter. Statistical analysis was performed using one-way ANOVA (***$P < 0.001$, **$P < 0.01$, *$P < 0.05$). Stars indicate the comparison of the GLV-1h68 group with the GLV-1h164 group (black), GLV-1h282 group (open), and GLV-1h442 group (gray).

in tumor volume was observed. Additionally, treatment of mice with GLV-1h282, expressing anti-FAP scAb, also exhibited significantly smaller tumor volume than treatment with GLV-1h68 (Figure 2c). Thus, an enhanced therapeutic effect on A549 tumor growth was observed on treatment of mice with GLV-1h164, GLV-1h442, or GLV-1h282, each expressing therapeutic antibodies, as compared with GLV-1h68. Moreover, the effect was superior to treatment with the therapeutic antibody alone and was either comparable or superior to the combination treatment of therapeutic antibody and GLV-1h68. A similar therapeutic effect was also observed in mice bearing DU145 tumor xenografts ($n = 5$) (Figure 2d).

Influences of intratumorally expressed antibodies targeting VEGF, EGFR, and FAP on the TME

The effect of virally expressed anti-VEGF scAb on tumor vasculature was evaluated in DU145 tumors excised on 36-day post injection (dpi) of VACV. Immunohistochemistry (IHC) staining of tumor sections was performed to assess blood vessel density (BVD), determined by counting CD31$^+$ blood vessels within tumor sections. The VACV infection was indicated by the fluorescence of virally expressed GFP (Figure 3a). The VACV colonization resulted in a dramatic reduction in BVD in the infected areas of tumors compared with both PBS-treated tumors and uninfected areas of the

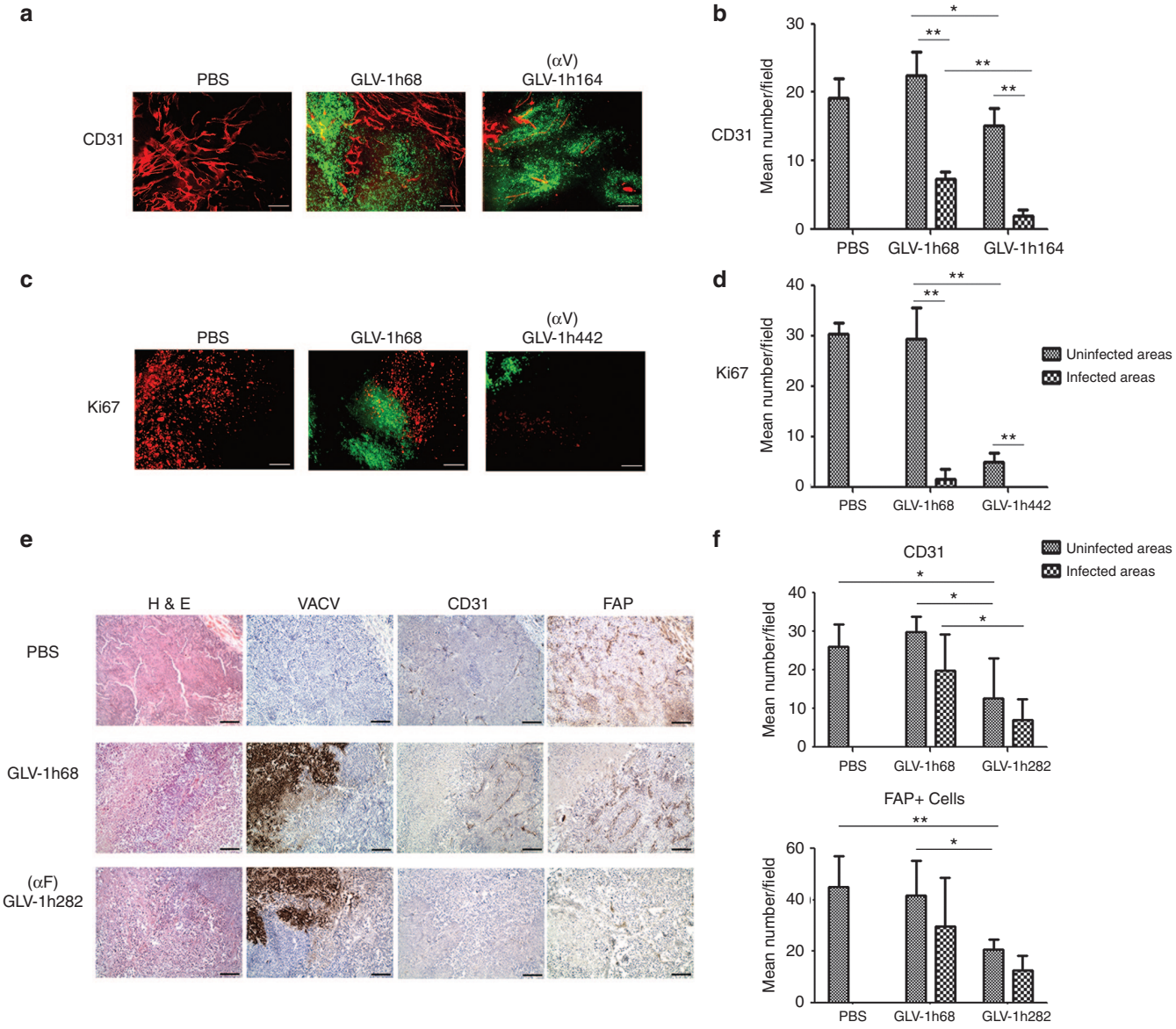

Figure 3 Influences of intratumorally expressed antibodies targeting VEGF, EGFP, and FAP on the TME. (**a**) Effect of virus treatment on tumor vasculature in DU145 tumors ($n = 3$). Sections were stained for CD31 expression (red). GFP expression (green) indicates virus infection. (**b**) Quantitative analysis of blood vessels was performed by counting CD31$^+$ blood vessels in eight non-overlapping microscopic fields per slide. Statistical analysis was performed with a two-tailed unpaired Student's *t*-test (**$P < 0.01$, *$P < 0.05$). (**c**) Effect of virus treatment on cell proliferation in DU145 tumors ($n = 3$). Sections were stained for Ki67 expression (red). GFP expression (green) indicates virus infection. Scale bars represent 1 mm in **a**, **c**. (**d**) Quantitative analysis of cell proliferation was performed by counting Ki67$^+$ cells in eight non-overlapping microscopic fields per slide. Statistical analysis was performed with a two-tailed unpaired Student's *t*-test (**$P < 0.01$, *$P < 0.05$). (**e**) Immunohistochemical characterization of viral replication and stromagenesis. Formalin-fixed and paraffin-embedded tumor tissues ($n = 4$–5 per group) were cut into 5-µm sections and H&E staining was performed. Adjacent sections were stained with anti-A27 for VACV, anti-CD31 for blood vessels and anti-FAP for FAP$^+$ stromal cells. (**f**) Bar graphs show mean numbers of CD31$^+$ cells and FAP$^+$ stromal clusters in infected or uninfected areas. CD31$^+$ and FAP$^+$ stromal clusters in five non-overlapping microscopic fields (100× magnification) per tumor were counted. Statistical analysis was performed with a two-tailed unpaired Student's *t*-test (**$P < 0.01$, *$P < 0.05$).

same tumors (Figure 3b). This was true for both GLV-1h68- and GLV-1h164-treated tumors. However, BVD in the uninfected areas of GLV-1h68-treated tumors was not significantly different from that in PBS-treated tumors. In contrast, treatment with GLV-1h164 significantly reduced BVD in the infected and uninfected areas of tumors compared with GLV-1h68-treated tumors. Thus, while VACV infection alone by GLV-1h68 reduced BVD in tumors, the effect was localized to the site of infection, whereas, the combination of VACV infection and expression of anti-VEGF scAb by GLV-1h164 not only further reduced BVD in the infected areas of tumors but also extended the effect to uninfected areas.

It is well known that overexpression of EGFR leads to uncontrolled cell growth.[7] IHC staining with anti-Ki67 was performed to assess whether virally expressed anti-EGFR nanobody suppressed cell proliferation in tumors. As expected, colonization of tumors with either GLV-1h68 or GLV-1h442, expressing anti-EGFR nanobody, greatly reduced the number of $Ki67^+$ cells in the infected areas compared with PBS-treated tumors (Figure 3c). Interestingly, the number of $Ki67^+$ cells in the uninfected areas of GLV-1h442-treated tumors was also significantly reduced compared with the uninfected areas of GLV-1h68-treated tumors (Figure 3d). This suggested that the anti-EGFR nanobody secreted from cells infected with GLV-1h442 also acted on uninfected cells, reducing their proliferation.

FAP is a mesenchymal stem cell (MSC) marker involved in angiogenesis.[31–33] The effect of intratumorally expressed anti-FAP scAb was evaluated by counting the FAP^+ cells and $CD31^+$ cells in FaDu tumors, which express high levels of FAP.[34] Although FaDu tumors did not respond to treatment with GLV-1h68, their growth was significantly inhibited by GLV-1h282 expressing anti-FAP scAb (Supplementary Figure S1). In GLV-1h68-colonized tumors, the numbers of $CD31^+$ cells and FAP+ cells were greatly reduced in the infected areas, whereas no effect was observed in the uninfected areas compared with PBS-treated tumors (Figure 3e,f). In contrast, the numbers of $CD31^+$ cells and FAP^+ cells in GLV-1h282-treated tumors were significantly reduced in both the infected and uninfected areas compared with GLV-1h68-treated tumors.

Construction of additional new recombinant VACVs expressing two antibodies targeting VEGF and EGFR or VEGF and FAP

Based on the positive effects of treatment with VACVs expressing single antibodies, additional new recombinant VACVs expressing two antibodies targeting VEGF and EGFR or VEGF and FAP were constructed. The expression cassette for anti-EGFR nanobody (anti-EGFRVHHFLAG) or anti-FAP scAb (GLAF-5) was inserted into the *J2R* locus of GLV-1h164, which also contained the anti-VEGF (GLAF-2) expression cassette, to replace the human norepinephrine transporter (hNET) expression cassette, resulting in GLV-1h444 and GLV-1h446, respectively (Figure 1b). To verify the expression of each antibody from the new recombinant VACVs, A549 cells were infected with the new VACV strains and cell lysates were analyzed by western blot. The results showed that the respective antibodies were expressed from each virus as intended (Supplementary Figure S2).

Virally expressed two antibodies do not show negative effects on viral replication efficiency

Viral replication assays were performed in A549 cells at a multiplicity of infection (MOI) of 0.01 (Supplementary Figure S3). The recombinant VACVs expressing single or two antibodies showed significantly higher replication efficiency than GLV-1h68 at 24-hour postinfection (hpi). However, there was no significant difference in the replication efficiency at 48 or 72 hpi. Similar results were obtained in DU145 cells. Thus, the expression of two antibodies in VACVs did not show negative effects on their overall replication efficiency in cell culture.

Virally expressed two antibodies targeting the TME further improve virotherapy

Encouraged by the results from the recombinant VACVs expressing single antibodies targeting the TME, we evaluated whether two antibodies expressed from the same VACV would further improve virotherapy. A single dose of each VACV strain was injected into mice bearing A549 tumor xenografts (Figure 4a,b). Control animals were treated with PBS or the combination of Avastin and Erbitux. The treatment with Avastin and Erbitux twice weekly for 5 weeks beginning at 10 dpi delayed tumor growth during the period of antibody treatment, but tumor growth resumed after the termination of antibody treatment. Interestingly, tumors in mice treated with GLV-1h444 or GLV-1h446, both expressing two antibodies, showed only minimal growth over the period of the experiment. In contrast, tumors in mice treated with VACVs expressing single antibodies initially grew as fast as or only slightly slower than tumors treated with PBS before tumor growth slowed significantly, followed by tumor shrinkage. Overall, the tumor volumes in mice treated with GLV-1h444 or GLV-1h446, expressing two antibodies, were less than the tumor volumes in mice treated with VACVs expressing single antibodies. The tumor growth curves of individual mice bearing A549 tumors are shown in Supplementary Figure S4. Similar patterns of tumor growth were obtained with DU145 tumors (Figure 4c).

Virally expressed antibodies are detectable in sera of treated mice

After the verification of antibody expression in virus-infected cells in culture, the presence of antibodies in tumor-bearing mice was also investigated. The blood samples were collected retro-orbitally from the same mice at 7, 21, and 35 dpi. All samples were tested for the presence of anti-FAP scAb with FAP-precoated plates, anti-EGFR nanobody with EGFR-precoated plates, and anti-VEGF scAb with VEGF-precoated plates. All of the antibodies were detectable at all three time points (Figure 4d–f). The expression of GLAF-2 was lower in mice treated with GLV-1h164 (single antibody) than in mice treated with GLV-1h444 and GLV-1h446 (two antibodies) at 7 and 21 dpi, consistent with the lower viral titers in tumors at 14 dpi in the GLV-1h164-treated group (Supplementary Table S1). Nonetheless, in all cases, the expression of antibodies at the early stages (day 7 and 21) coincided with low tumor volumes and at the later stage (day 35) preceded tumor shrinkage.

Virally expressed two antibodies do not alter viral distribution and toxicity in mice

The possible adverse effect of antibody-expressing VACV administration in mice was evaluated by assessing the change in net body weight over the course of treatment. In both A549 and DU145 tumor xenograft models, no significant change in the mean net body weight was observed for any of the treated or control groups (Supplementary Figure S5a–c). Also evaluated was the viral biodistribution in different organs and tumors in A549 tumor-bearing mice at 14 dpi as determined by standard viral plaque assays (Supplementary Table S1). Significant viral titers were detected in all treated tumors and no or minimal titers were detected in other organs. The viral titers in tumors treated with GLV-1h282,

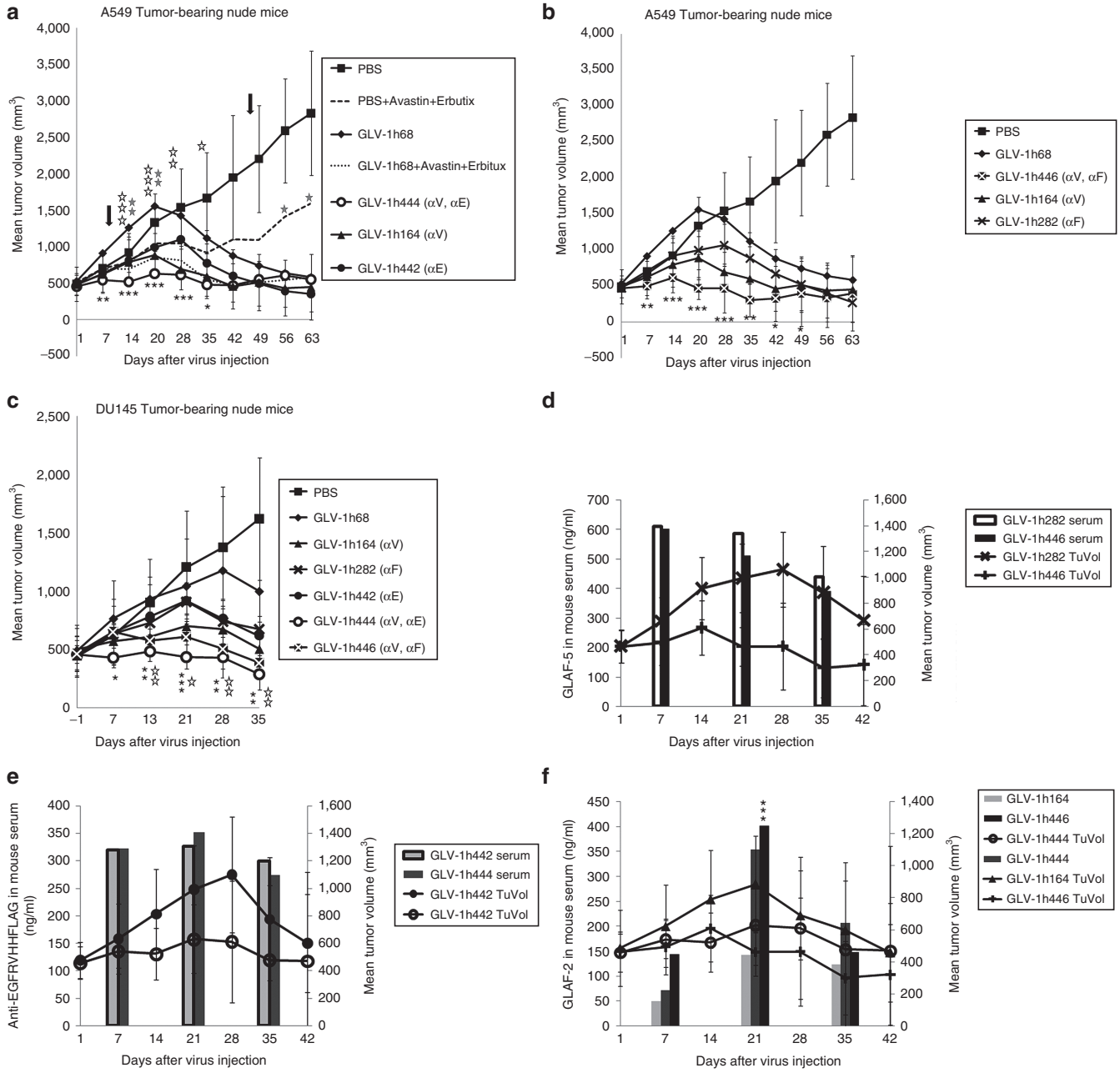

Figure 4 Virally expressed two therapeutic antibodies targeting the TME further improve virotherapy. (**a**) Enhanced therapeutic effects of GLV-1h444 in A549 tumor-bearing nude mice. Mice ($n \geq 7$) were treated with virus alone, Avastin+Erbitux, PBS alone, or virus in combination with Avastin and Erbitux. A single dose of virus (2×10^6 pfu/mouse) was given i.v. when tumor volumes reached 450 mm^3. Avastin and Erbitux were administered i.p. at doses of 5 mg/kg and 3 mg/kg, respectively, twice per week for 5 weeks, starting at 10 dpi. The arrows indicate the beginning and end of Avastin and Erbitux treatment. Statistical analysis was performed using one-way ANOVA (***$P < 0.001$, **$P < 0.01$, *$P < 0.05$). Stars indicate the comparison of the GLV-1h68 group with the GLV-1h444 group (black), the GLV-1h68+Avastin+Erbitux group (open), and the PBS+Avastin+Erbitux group (gray). (**b**) Enhanced therapeutic effects of GLV-1h446 compared with its parental viruses in A549 tumor-bearing nude mice. Mice ($n \geq 7$) were i.v. injected with each VACV strain alone at a dose of 2×10^6 pfu/mouse when tumor volumes reached 450 mm^3. Statistical analysis was performed using one-way ANOVA (***$P < 0.001$, **$P < 0.01$, *$P < 0.05$). Stars indicate the comparison of the GLV-1h68 group with the GLV-1h446 group (black). (**c**) Enhanced therapeutic effects of GLV-1h444 and GLV-1h446 compared with their parental viruses in DU145 tumor-bearing mice. Mice ($n = 5$) were injected i.v. with each VACV strain alone at a dose of 2×10^6 pfu/mouse when tumor volumes reached 450 mm^3. Statistical analysis was performed using one-way ANOVA (***$P < 0.001$, **$P < 0.01$, *$P < 0.05$). Stars indicate the comparison of the GLV-1h68 group with the GLV-1h444 group (black) and with the GLV-1h446 group (open). (**d–f**) Detection of antibodies in mice sera and the change of tumor volumes in mice bearing A549 tumors after VACV treatment. Blood samples were collected retro-orbitally at 7, 21, and 35 dpi. The concentration of antibodies in mice sera was determined by ELISA with precoated FAP, EGFR, and VEGF plates. Tumors were measured with a digital caliper. Statistical analysis was performed with a two-tailed unpaired Student's *t*-test (***$P < 0.001$).

expressing anti-FAP scAb, and GLV-1h442, expressing anti-EGFR nanobody, were higher than in tumors treated with GLV-1h68, although not statistically significant, whereas the viral titer of GLV-1h164, expressing anti-VEGF scAb, in tumors was significantly lower than the other virus strains (GLV-1h164 versus GLV-1h68, $P = 0.02$, and versus GLV-1h446, $P = 0.04$).

Effects of intratumorally expressed two antibodies targeting VEGF and EGFR or VEGF and FAP on the TME

The influence of virally expressed two antibodies on the TME was evaluated by examining cell proliferation and BVD in DU145 tumor xenografts by staining tumor sections obtained at 36 dpi with anti-Ki67 and anti-CD31 antibodies. The VACV infection was confirmed by GFP fluorescence. The representative images of IHC staining of proliferating Ki67$^+$ cells are shown in Figure 5a. In the infected areas of the tumors, Ki67$^+$ cells were significantly reduced after treatment with any of the VACV strains, including GLV-1h68 (Figure 5c). In the uninfected areas of VACV-treated tumors, Ki67$^+$ cells were significantly reduced only after treatment with the single anti-EGFR nanobody-expressing VACV, GLV-1h442, and the two antibody-expressing VACVs, GLV-1h444 and GLV-1h446 (Figure 5b).

The images of DU145 tumor sections stained with anti-CD31 antibody showed that the infected areas of tumors were significantly reduced in BVD compared with the uninfected areas regardless of the VACV used for treatment (Figure 6a–c). Compared with GLV-1h68, a significant further reduction in BVD was observed with VACVs expressing anti-VEGF antibody (GLAF-2), either singly or in combination with the other antibody. As expected, BVD in tumors treated with GLV-1h442, expressing anti-EGFR but not anti-VEGF, was not significantly different than that in tumors treated with GLV-1h68, but the infected areas treated with GLV-1h444 and GLV-1h446 showed a further reduced BVD.

DISCUSSION

We report here that new recombinant VACVs expressing antibodies targeting VEGF, EGFR, and FAP singly and in combination significantly enhanced oncolytic virotherapy in preclinical animal models. The therapeutic efficacy of GLV-1h164, GLV-1h442, and GLV-1h282, each expressing a scAb, was significantly better than that of their parental virus GLV-1h68, indicating that oncolytic virotherapy can be improved by viral expression of individual antibodies against VEGF to reduce angiogenesis, EGFR to suppress cell proliferation, or FAP to reduce angiogenesis and suppress recruitment of MSCs. Moreover, the therapeutic efficacy was further enhanced by expressing two antibodies in one VACV strain. The therapeutic efficacy of GLV-1h444 that expresses antibodies targeting both VEGF and EGFR was significantly better than that of the combination treatment with Avastin and Erbitux and was also superior to treatment with GLV-1h68 in combination with Avastin and Erbitux.

The high-level expression of VEGF, EGFR, and FAP in tumors is associated with poor prognosis.[6,7,23,25,35,36] Despite promising results in preclinical trials,[37,38] Avastin and Erbitux have shown only limited clinical efficacy,[8–10] partially owing to the poor penetration and low tumor targeting of the antibodies as well as rapid clearance from the circulation after systemic administration.[11] The oncolytic VACV not only specifically targets and destroys tumor cells but also mediates local production of therapeutic proteins in colonized tumors,[28,29] thus

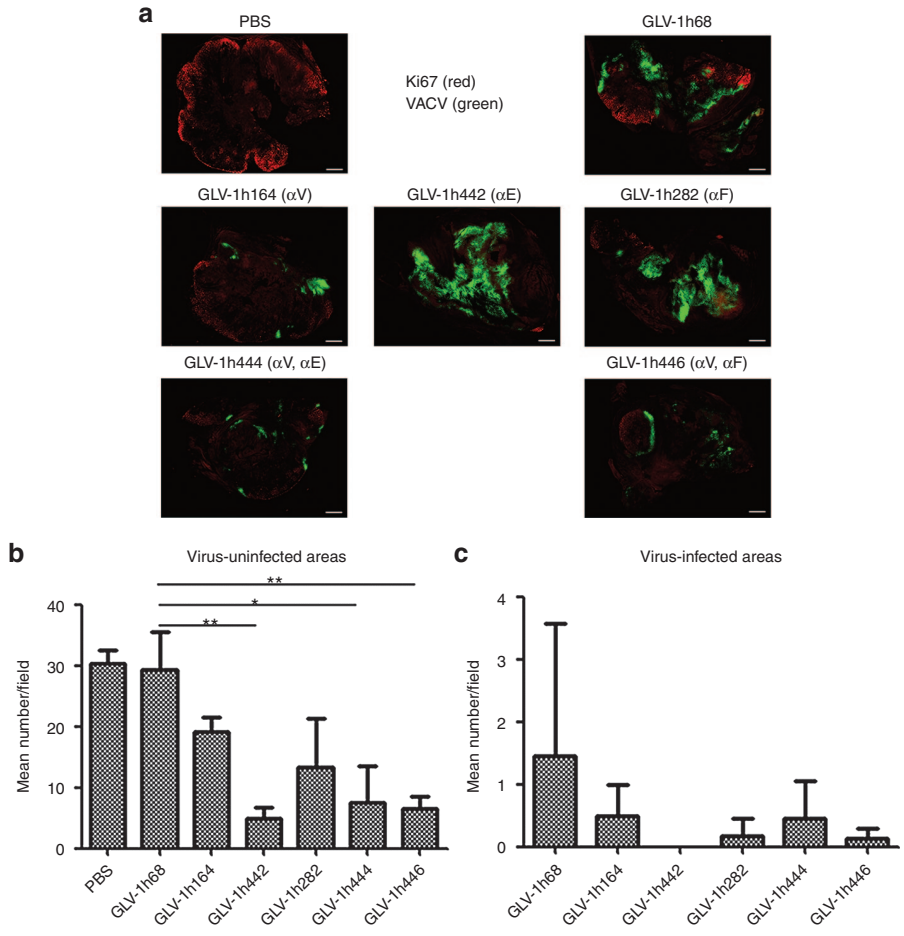

Figure 5 Virally expressed two antibodies by GLV-1h444 and GLV-1h446 contribute to the suppression of cell proliferation in tumors. (**a**) Suppression of cell proliferation by VACVs in DU145 tumors ($n = 3$). GFP expression (green) indicates virus infection. Cell proliferation was examined by staining with anti-Ki67 antibody (red). Scale bars = 1mm. (**b, c**) Quantitative analysis of cell proliferation in uninfected or infected areas was performed by counting Ki67$^+$ cells in eight non-overlapping microscopic fields per slide. Statistical analysis was performed using a two-tailed unpaired Student's *t*-test (**$P < 0.01$, *$P < 0.05$).

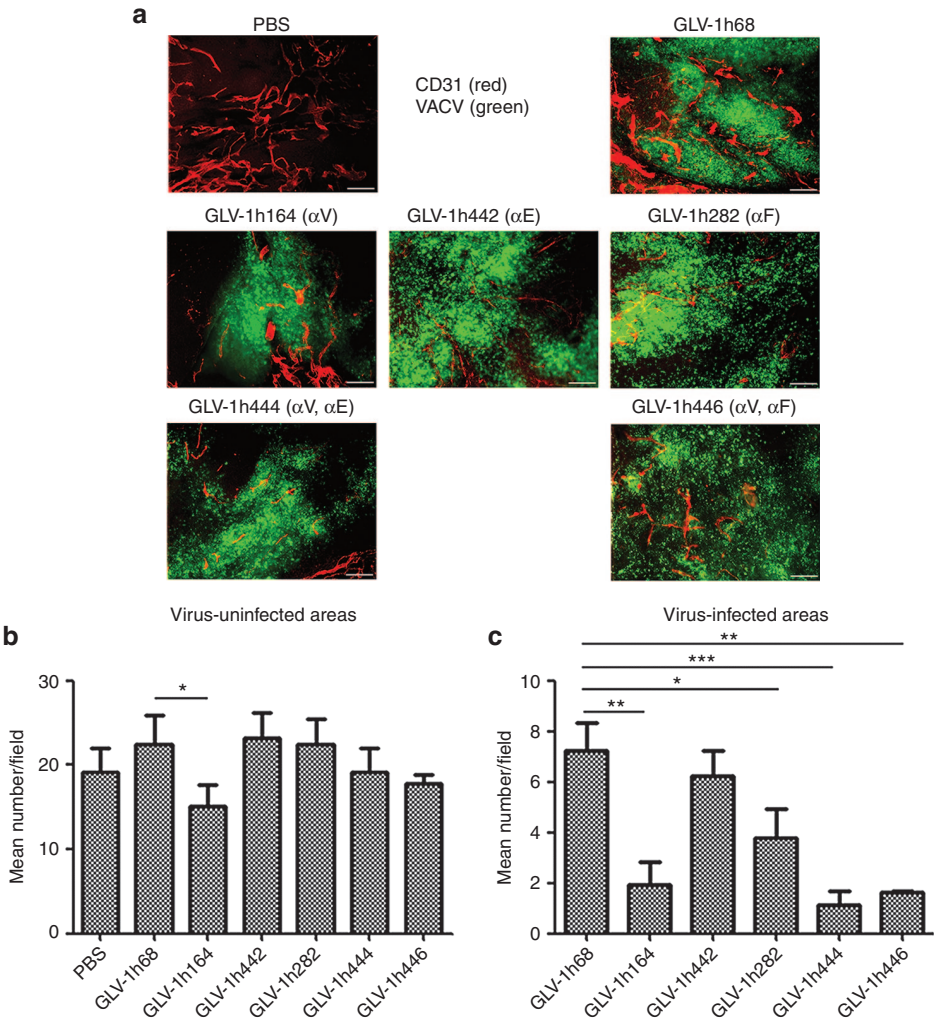

Figure 6 Virally expressed two antibodies by GLV-1h444 and GLV-1h446 contribute to the suppression of angiogenesis in tumors. (**a**) Reduced tumor vasculature by VACVs in DU145 tumors ($n = 3$). Sections were stained with anti-CD31 antibody (red). GFP expression (green) indicates virus infection. (**b, c**) uantitative analysis of blood vessels in uninfected or infected areas was performed by counting $CD31^+$ cells in eight non-overlapping microscopic fields per slide. Statistical analysis was performed using a two-tailed unpaired Student's *t*-test (***$P < 0.001$, **$P < 0.01$, *$P < 0.05$). Scale bars indicate 1 mm in **a**.

circumventing the limitations associated with the use of antibody therapeutics. The continuous presence of antibodies was demonstrated in the sera of mice treated with VACVs expressing single or two antibodies. The antibodies were detected in higher amounts in the early phase (7 and 21 dpi) than in the later phase (35 dpi) following injection of the virus when tumors had already started to shrink. In addition, anti-FAP (GLAF-5) and anti-EGFRVHHFLAG antibodies occurred in higher amounts in the sera of mice treated with GLV-1h282 and GLV-1h442, respectively, than was anti-VEGF (GLAF-2) antibody in the sera of mice treated with GLV-1h164. This was consistent with the higher viral titers of GLV-1h282 and GLV-1h442 than GLV-1h164 in tumors. Although the viral titer of GLV-1h68 in tumors was significantly higher than that of GLV-1h164 ($P = 0.02$), GLV-1h164 replicated slightly faster than GLV-1h68 in culture, suggesting that the expression of GLAF-2 decreased viral replication in tumors. It is possible that the suppression of blood vessels by anti-VEGF limited nutrient supply to tumors and changed the TME, which not only resulted in reduced tumor growth but also decreased viral replication. The expression of the antibodies targeting EGFR or FAP had no negative effect on viral replication in tumors.

It is well known that cancer progression is due to uncontrolled growth of cancer cells. Treatment with GLV-1h68 suppressed cell proliferation in tumors, evident in the dramatic decrease in the number of Ki67+ cells in the infected areas, consistent with the intrinsic property of VACV infection. Notably, treatment with GLV-1h442 and GLV-1h444, expressing anti-EGFR nanobody, significantly reduced the number of $Ki67^+$ cells not only in the infected areas but also in the uninfected areas, suggesting that the anti-EGFR nanobody secreted from the infected cells spread into uninfected areas, suppressing the proliferation of $EGFR^+$ cells. Although treatment with GLV-1h164, expressing anti-VEGF antibody, or GLV-1h282, expressing anti-FAP antibody, significantly suppressed proliferation in the infected areas of the tumor, the effect was only slight, but not significant, in the uninfected areas. Importantly, treatment with GLV-1h446, expressing both anti-VEGF and anti-FAP, significantly suppressed proliferation in both the infected and uninfected areas, demonstrating the added inhibitory effect of two antibody expressions on cell growth.

Cancer growth and development also require continuous supply of nutrients through blood vessels.[2,39] A reduction of BVD was observed in the infected areas, but not in the uninfected areas of GLV-1h68-colonized tumors, suggesting that VACV infection itself can lead to the destruction of tumor vasculature.[40] The expression of anti-VEGF scAb not only enhanced blood vessel destruction in the infected areas but also caused a significant decrease in BVD in the

uninfected areas. Thus, like anti-EGFR nanobody, anti-VEGF scAb can also spread from infected areas to uninfected areas. Therapies targeting FAP inhibit tumor growth partially through suppressing tumor angiogenesis.[33,41,42] Virally expressed anti-FAP scAb significantly decreased BVD in both the infected and uninfected areas in the FaDu tumor xenograft model, and in the infected areas in the DU145 tumor xenograft model. Although the expression of the anti-EGFR nanobody did not significantly affect BVD in either infected or uninfected areas in the DU145 tumor xenograft model, it has been reported that EGFR promotes tumor angiogenesis.[43]

FAP is one of the markers expressed by cancer-associated fibroblasts (CAFs) that support tumor growth. The ablation of FAP+ CAFs was shown to suppress tumor growth.[44] Treatment of mice bearing FaDu tumor xenografts with GLV-1h282, expressing anti-FAP scAb, resulted in a great reduction in the number of FAP+ cells in both the infected and uninfected areas of the tumor compared with treatment with GLV-1h68. The enhanced antitumor effects of GLV-1h282 are likely attributed to an effect on CAFs, rather than on the cancer cells, since FaDu tumor cells do not express FAP.[34]

In summary, we have shown that oncolytic VACV infection itself greatly reduced cell proliferation and vascularity of colonized tumors. These antitumor effects were enhanced significantly by the expression of scAbs against VEGF, EGFR, and FAP in recombinant VACVs either singly or in combination. The effects of coexpression of the antibody or antibodies were either comparable or superior to the treatment with VACV combined with the clinical antibodies, with the benefit of single administration and localized delivery intratumorally. The therapeutic effect combined viral oncolysis of the infected tumor cells with antitumor alterations of the TME. To our knowledge, this is the first report demonstrating that virally expressed antibodies against EGFR and FAP singly enhanced oncolytic virotherapy and, in combination with anti-VEGF antibody, further improved antitumor therapeutic efficacy. Our findings suggest that the expression of antibodies targeting multiple pathways in the TME is an effective way to improve oncolytic virotherapy.

MATERIALS AND METHODS

Cell lines

African green monkey kidney fibroblasts CV-1, human lung carcinoma A549, hypopharyngeal carcinoma cell line FaDu, and human prostate cancer cell line DU145 were obtained from the American Type Culture Collection (Manassas, VA). CV-1 cells were cultured in Dulbecco's modified Eagle medium (DMEM); A549 cells were cultured in RPMI 1640; and FaDu and DU145 were cultured in Eagle's minimal essential medium. All media were supplemented with 10% fetal bovine serum (Cellgro, Manassas, VA).

Construction of plasmids and expression of antibodies

The parental triple-mutant VACV GLV-1h68 was constructed as described previously.[28] Briefly, it contains three foreign gene-expression cassettes encoding *Renilla* luciferase-*Aequorea* GFP fusion protein (RUC-GFP), β-galactosidase, and β-glucuronidase integrated into the *F14.5L*, *J2R*, and *A56R* loci of the Lister strain from the Institute of Viral Preparations (Moscow, Russia) viral genome, respectively.[28] The sequence of GLAF-5 was designed as described previously,[29] and was synthesized by GENEART-Invitrogen (Carlsbad, CA). The DYKDDDDK tag (gac tac aag gat gac gac gac aag) was added into the C-terminal coding region of anti-EGFRVHH,[13] resulting in anti-EGFRVHHFLAG. The DNA fragments were cloned into plasmids pCR-TK-P_{SEL} with the *Sal* I and *Pac* I sites, resulting in the plasmids pCR-TK-P_{SEL} (*GLAF-5*) and pCR-TK-P_{SEL} (*anti-EGFRVHHFLAG*), which were used for homologous recombination into the *J2R* locus in GLV-1h68 through double-reciprocal crossover, resulting in GLV-1h282 and GLV-1h442, respectively. GLV-1h446 and GLV-1h444 were generated similarly using the same plasmids and GLV-1h164 as the parental virus.[30] The recombinant VACVs were sequence-confirmed. All VACVs were propagated in CV-1 cells and purified through sucrose gradients by a standard protocol.[45]

For the detection of expression of antibodies, the cell samples were harvested at 24 hours after infection with each VACV strain at an MOI of 1, separated by 12% sodium dodecyl sulfate polyacrylamide gel electrophoresis (Invitrogen). The following antibodies were used: anti-DDDDK antibody (Abcam, Cambridge, MA) for the detection of FLAG tag, the custom-made antibody G6 for the detection of scAbs, and anti-A27 antibody (GenScript Corporation, Piscataway, NJ) for the detection of the membrane protein of VACV.

The concentrations of the antibodies in mice sera were determined in standard enzyme-linked immunosorbent assay (ELISA) using the commercial recombinant human EGFR (Abnova, Taipei, Taiwan), FAP (R&D Systems, Minneapolis, MN), and VEGF (Sigma, St. Louis, MO), as previously described.[29]

Viral replication assay

The cells were infected with VACVs at an MOI of 0.01 and the samples were harvested in triplicate at each time point after infection.

Animal studies

Five- to six-week-old nude male mice (Hsd:athymic Nude-*Foxn1nu* mice) were purchased from Harlan (Livermore, CA) and were cared for and maintained under the protocol approved by the Institutional Animal Care and Use Committee of Explora Biolabs (San Diego Science Center, San Diego, CA).

1×10^6 of FaDu, 5×10^6 of A549, or 1×10^7 of DU145 cells were subcutaneously implanted into the right hind leg of mice. The tumor volumes were measured weekly in three dimensions using a digital caliper and were calculated as ((length × width × (height − 5))/2), and body weights were measured weekly. The net body weight for each animal was calculated by subtracting the total body weight at each time point from the weight of the tumor (assuming a tumor density of 1 g/cc). The percent change in net body weight was the difference between the net body weight of each animal at a specific time point and its net body weight immediately prior to treatment divided by the net body weight immediately prior to treatment, expressed as a percentage. A single dose of 2×10^6 pfu/mouse (unless otherwise specified) in 100-µl PBS of each VACV strain was administered by retro-orbital injection when the tumor volume reached ~450 mm^3. Hundred microliters of PBS were injected as a negative control.

For treatment with therapeutic antibodies, mice were intraperitoneally (i.p.) injected with Avastin (5 mg/kg) and/or Erbitux (3 mg/kg) twice weekly for 5 weeks starting at 10 dpi.

The tumors and organs were excised and homogenized using a MagNA Lyser (Roche Diagnostics, Indianapolis, IN). The viral titers were determined in CV-1 cells by standard plaque assays.

Histological analysis

FaDu tumors were excised and paraffin-embedded, followed by the standard dehydration process.[41] The tumor samples were cut into 5-µm sections and stained with hematoxylin and eosin (H&E). The sections were dewaxed and antigen retrieval was performed in a sodium citrate buffer. The following antibodies were used: anti-FAP (Abcam) and anti-A27 (GenScript Corporation). Biotinylated secondary antibodies (goat anti-rabbit; Jackson ImmunoResearch Laboratories, Suffolk, UK) were used and detection was performed with Vectorstain Elite ABC reagent and Vector ImmPact DAB Peroxidase substrate (Vector Laboratories, Burlingame, CA).

DU145 tumors were excised at 36 dpi, followed by paraformaldehyde fixation, and then cut into 100-µm sections. The blood vessels and cell proliferation were detected with anti-CD31 antibody (BD Pharmingen, San Jose, CA) and anti-Ki67 antibody (BD Pharmingen), respectively.

The examination of tumor sections was conducted with an MZ16 FA fluorescence stereomicroscope (Leica, Buffalo Grove, IL) equipped with a digital charge-coupled device camera (Leica). Digital images (1,300 to 1,030-pixel images) were processed using Adobe Photoshop 7.0 software (San Jose, CA).

Statistical analysis

The statistical significance of differences between groups of animals was analyzed using a two-tailed unpaired Student's *t*-test (Excel 2003; Microsoft, Redmond, WA) or one-way analysis of variance (ANOVA) in STATISTICS. A P-value <0.05 was considered significant.

ACKNOWLEDGMENTS

We thank Terry Trevino, Jason Aguilar, and Melody Fells for excellent technical support, Ying Wang (Shanghai Institute of Immunology, Institute of Medical Science, Shanghai

Jiaotong University School of Medicine, China) for the generous gift of the plasmid pGH-anti-EGFRVHH. We also would like to thank Joseph Cappello for editorial help. This work was supported by a research grant from Genelux Corporation (R&D facility in San Diego, CA, USA). T.H., a visiting graduate student from Szalay's laboratory in the Institute of Biochemistry, University of Würzburg, Germany, was supported by a graduate stipend and foreign travel grant from Genelux Corporation. The authors would like to thank DFG and the University of Wuerzburg library publication support program and the Margot and Aladar Szalay family trust fund for their generous help with the publication costs.

CONFLICT OF INTEREST

H.W., N.G.C., A.F., B.M., and A.A.S. are salaried employees of Genelux Corporation and have personal financial interests at Genelux Corporation. No competing financial interests exist for T.H.

REFERENCES

1. Tlsty, TD and Coussens, LM (2006). Tumor stroma and regulation of cancer development. *Annu Rev Pathol* **1**: 119–150.
2. Pietras, K and Ostman, A (2010). Hallmarks of cancer: interactions with the tumor stroma. *Exp Cell Res* **316**: 1324–1331.
3. Ferrara, N, Hillan, KJ, Gerber, HP and Novotny, W (2004). Discovery and development of bevacizumab, an anti-VEGF antibody for treating cancer. *Nat Rev Drug Discov* **3**: 391–400.
4. Puré, E (2009). The road to integrative cancer therapies: emergence of a tumor-associated fibroblast protease as a potential therapeutic target in cancer. *Expert Opin Ther Targets* **13**: 967–973.
5. Herbst, RS (2004). Review of epidermal growth factor receptor biology. *Int J Radiat Oncol Biol Phys* **59**(suppl. 2): 21–26.
6. Meadows, KL and Hurwitz, HI (2012). Anti-VEGF therapies in the clinic. *Cold Spring Harb Perspect Med* **2**: 1–27.
7. Nicholson, RI, Gee, JM and Harper, ME (2001). EGFR and cancer prognosis. *Eur J Cancer* **37** (suppl. 4): S9–15.
8. Bergers, G and Hanahan, D (2008). Modes of resistance to anti-angiogenic therapy. *Nat Rev Cancer* **8**: 592–603.
9. Karapetis, CS, Khambata-Ford, S, Jonker, DJ, O'Callaghan, CJ, Tu, D, Tebbutt, NC *et al*. (2008). K-ras mutations and benefit from cetuximab in advanced colorectal cancer. *N Engl J Med* **359**: 1757–1765.
10. Alberts, SR, Sargent, DJ, Nair, S, Mahoney, MR, Mooney, M, Thibodeau, SN *et al*. (2012). Effect of oxaliplatin, fluorouracil, and leucovorin with or without cetuximab on survival among patients with resected stage III colon cancer: a randomized trial. *JAMA* **307**: 1383–1393.
11. Jain, RK (2001). Delivery of molecular and cellular medicine to solid tumors. *Adv Drug Deliv Rev* **46**: 149–168.
12. Liang, WC, Wu, X, Peale, FV, Lee, CV, Meng, YG, Gutierrez, J *et al*. (2006). Cross-species vascular endothelial growth factor (VEGF)-blocking antibodies completely inhibit the growth of human tumor xenografts and measure the contribution of stromal VEGF. *J Biol Chem* **281**: 951–961.
13. Bell, A, Wang, ZJ, Arbabi-Ghahroudi, M, Chang, TA, Durocher, Y, Trojahn, U *et al*. (2010). Differential tumor-targeting abilities of three single-domain antibody formats. *Cancer Lett* **289**: 81–90.
14. Iqbal, U, Trojahn, U, Albaghdadi, H, Zhang, J, O'Connor-McCourt, M, Stanimirovic, D *et al*. (2010). Kinetic analysis of novel mono- and multivalent VHH-fragments and their application for molecular imaging of brain tumours. *Br J Pharmacol* **160**: 1016–1028.
15. Dumoulin, M, Conrath, K, Van Meirhaeghe, A, Meersman, F, Heremans, K, Frenken, LG *et al*. (2002). Single-domain antibody fragments with high conformational stability. *Protein Sci* **11**: 500–515.
16. Cortez-Retamozo, V, Lauwereys, M, Hassanzadeh Gh, G, Gobert, M, Conrath, K, Muyldermans, S *et al*. (2002). Efficient tumor targeting by single-domain antibody fragments of camels. *Int J Cancer* **98**: 456–462.
17. Gottlin, EB, Xiangrong Guan, Pegram, C, Cannedy, A, Campa, MJ and Patz, EF Jr (2009). Isolation of novel EGFR-specific VHH domains. *J Biomol Screen* **14**: 77–85.
18. Roovers, RC, Laeremans, T, Huang, L, De Taeye, S, Verkleij, AJ, Revets, H *et al*. (2007). Efficient inhibition of EGFR signaling and of tumour growth by antagonistic anti-EFGR nanobodies. *Cancer Immunol Immunother* **56**: 303–317.
19. Huang, L, Gainkam, LO, Caveliers, V, Vanhove, C, Keyaerts, M, De Baetselier, P *et al*. (2008). SPECT imaging with 99mTc-labeled EGFR-specific nanobody for *in vivo* monitoring of EGFR expression. *Mol Imaging Biol* **10**: 167–175.
20. Mathew, S, Scanlan, MJ, Mohan Raj, BK, Murty, VV, Garin-Chesa, P, Old, LJ *et al*. (1995). The gene for fibroblast activation protein alpha (FAP), a putative cell surface-bound serine protease expressed in cancer stroma and wound healing, maps to chromosome band 2q23. *Genomics* **25**: 335–337.
21. Niedermeyer, J, Enenkel, B, Park, JE, Lenter, M, Rettig, WJ, Damm, K *et al*. (1998). Mouse fibroblast-activation protein–conserved Fap gene organization and biochemical function as a serine protease. *Eur J Biochem* **254**: 650–654.
22. Park, JE, Lenter, MC, Zimmermann, RN, Garin-Chesa, P, Old, LJ and Rettig, WJ (1999). Fibroblast activation protein, a dual specificity serine protease expressed in reactive human tumor stromal fibroblasts. *J Biol Chem* **274**: 36505–36512.
23. Gorrell, MD, Wang, XM, Levy, MT, Kable, E, Marinos, G, Cox, G *et al*. (2003). Intrahepatic expression of collagen and fibroblast activation protein (FAP) in hepatitis C virus infection. *Adv Exp Med Biol* **524**: 235–243.
24. Ge, Y, Zhan, F, Barlogie, B, Epstein, J, Shaughnessy, J Jr and Yaccoby, S (2006). Fibroblast activation protein (FAP) is upregulated in myelomatous bone and supports myeloma cell survival. *Br J Haematol* **133**: 83–92.
25. Wikberg, ML, Edin, S, Lundberg, IV, Van Guelpen, B, Dahlin, AM, Rutegård, J *et al*. (2013). High intratumoral expression of fibroblast activation protein (FAP) in colon cancer is associated with poorer patient prognosis. *Tumour Biol* **34**: 1013–1020.
26. Zhang, J, Valianou, M, Simmons, H, Robinson, MK, Lee, HO, Mullins, SR *et al*. (2013). Identification of inhibitory scFv antibodies targeting fibroblast activation protein utilizing phage display functional screens. *FASEB J* **27**: 581–589.
27. Brocks, B, Garin-Chesa, P, Behrle, E, Park, JE, Rettig, WJ, Pfizenmaier, K *et al*. (2001). Species-crossreactive scFv against the tumor stroma marker "fibroblast activation protein" selected by phage display from an immunized FAP-/- knock-out mouse. *Mol Med* **7**: 461–469.
28. Zhang, Q, Yu, YA, Wang, E, Chen, N, Danner, RL, Munson, PJ *et al*. (2007). Eradication of solid human breast tumors in nude mice with an intravenously injected light-emitting oncolytic vaccinia virus. *Cancer Res* **67**: 10038–10046.
29. Frentzen, A, Yu, YA, Chen, N, Zhang, Q, Weibel, S, Raab, V *et al*. (2009). Anti-VEGF single-chain antibody GLAF-1 encoded by oncolytic vaccinia virus significantly enhances antitumor therapy. *Proc Natl Acad Sci USA* **106**: 12915–12920.
30. Buckel, L, Advani, SJ, Frentzen, A, Zhang, Q, Yu, YA, Chen, NG *et al*. (2013). Combination of fractionated irradiation with anti-VEGF expressing vaccinia virus therapy enhances tumor control by simultaneous radiosensitization of tumor associated endothelium. *Int J Cancer* **133**: 2989–2999.
31. Tran, E, Chinnasamy, D, Yu, Z, Morgan, RA, Lee, CC, Restifo, NP *et al*. (2013). Immune targeting of fibroblast activation protein triggers recognition of multipotent bone marrow stromal cells and cachexia. *J Exp Med* **210**: 1125–1135.
32. Roberts, EW, Deonarine, A, Jones, JO, Denton, AE, Feig, C, Lyons, SK *et al*. (2013). Depletion of stromal cells expressing fibroblast activation protein-a from skeletal muscle and bone marrow results in cachexia and anemia. *J Exp Med* **210**: 1137–1151.
33. Liao, D, Luo, Y, Markowitz, D, Xiang, R and Reisfeld, RA (2009). Cancer associated fibroblasts promote tumor growth and metastasis by modulating the tumor immune microenvironment in a 4T1 murine breast cancer model. *PLoS ONE* **4**: e7965.
34. Ostermann, E, Garin-Chesa, P, Heider, KH, Kalat, M, Lamche, H, Puri, C *et al*. (2008). Effective immunoconjugate therapy in cancer models targeting a serine protease of tumor fibroblasts. *Clin Cancer Res* **14**: 4584–4592.
35. Chang, JH, Garg, NK, Lunde, E, Han, KY, Jain, S and Azar, DT (2012). Corneal neovascularization: an anti-VEGF therapy review. *Surv Ophthalmol* **57**: 415–429.
36. Mamot, C and Rochlitz, C (2006). Targeting the epidermal growth factor receptor (EGFR)–a new therapeutic option in oncology? *Swiss Med Wkly* **136**: 4–12.
37. Vincenzi, B, Schiavon, G, Silletta, M, Santini, D and Tonini, G (2008). The biological properties of cetuximab. *Crit Rev Oncol Hematol* **68**: 93–106.
38. Manegold, C (2008). Bevacizumab for the treatment of advanced non-small-cell lung cancer. *Expert Rev Anticancer Ther* **8**: 689–699.
39. Xing, F, Saidou, J and Watabe, K (2010). Cancer associated fibroblasts (CAFs) in tumor microenvironment. *Front Biosci (Landmark Ed)* **15**: 166–179.
40. Kirn, DH and Thorne, SH (2009). Targeted and armed oncolytic poxviruses: a novel multi-mechanistic therapeutic class for cancer. *Nat Rev Cancer* **9**: 64–71.
41. Santos, AM, Jung, J, Aziz, N, Kissil, JL and Puré, E (2009). Targeting fibroblast activation protein inhibits tumor stromagenesis and growth in mice. *J Clin Invest* **119**: 3613–3625.
42. Cai, F, Peng, F, Wang, C, Li, Z, Xian, S and Wei, Y (2012). Effect of Short Hairpin RNA Targeting of Fibroblast Activation Protein on Tumor Growth and Angiogenesis in a 4T1 Murine Breast Cancer Model. 2012 ASCO Annual Meeting, Chicago, IL, 1–5 June 2012.
43. Ellis, LM (2004). Epidermal growth factor receptor in tumor angiogenesis. *Hematol Oncol Clin North Am* **18**: 1007–21, viii.
44. Kakarla, S, Chow, KK, Mata, M, Shaffer, DR, Song, XT, Wu, MF *et al*. (2013). Antitumor effects of chimeric receptor engineered human T cells directed to tumor stroma. *Mol Ther* **21**: 1611–1620.
45. Joklik, WK (1962). The purification of four strains of poxvirus. *Virology* **18**: 9–18.

Supplementary Information accompanies this paper on the *Molecular Therapy—Oncolytics* website (http://www.nature.com/mto)